IRANIAN JOURNAL OF CATALYSIS

Nanosized mesoporous composite PW$_{12}$-APTES@KIT-6: An efficient heterogeneous catalyst for selective oxidation of sulfides to sulfoxides and sulfones

Razieh Fazaeli[*a], Hamid Aliyan[b], Somaieh Parishani Foroushani[a], Zahra Mohagheghian[a], Zahra Heidari[a]

[a]*Department of Chemistry, Shahreza Branch, Islamic Azad University, 86145-311, Iran.*
[b]*Department of Chemistry, Mobarakeh Branch, Islamic Azad University, 84815-119, Iran.*

ABSTRACT

Surface of mesostructured silica, KIT-6, was modified by grafting 3-aminopropyl-triethoxysilane (APTES) to have the positive charge, and thus, to provide sites for the immobilization of $H_3PW_{12}O_{40}$ (PW$_{12}$). This modified-nanosized mesoporous silica (PW$_{12}$-APTES@ KIT-6) was characterized by FTIR, XRD, BET and TEM. The oxidation of sulfides occurs effectively and selectively with H_2O_2 as the oxidant. PW$_{12}$-APTES@KIT-6 was used as the catalyst. The catalyst can be reused for several times but it will be less active.

Keywords: *Mesoporous silica KIT-6; Heterogeneous catalysis; Polyoxotungstate.*
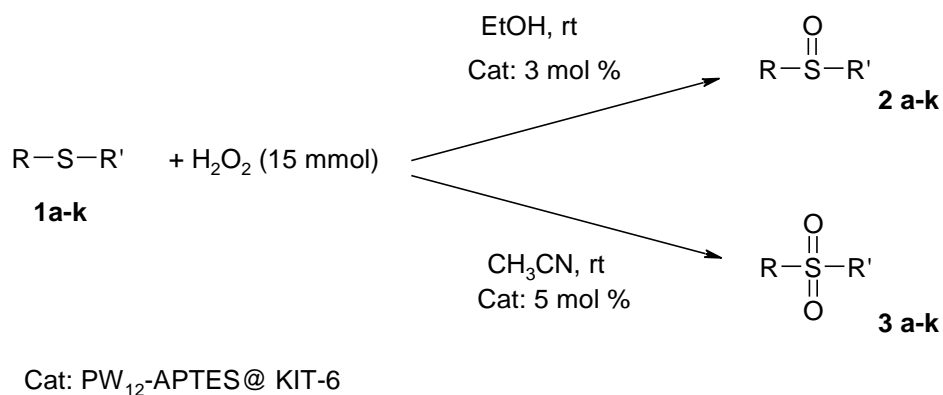
1. Introduction

Ordered mesoporous silicas, due to their high specific surface areas, high pore volumes and narrow pore size distributions have been reported as suitable supports for various metal and metal-oxide nanoparticles [1-5]. These possibilities have been essentially expanded with the application of poly(alkylene oxide) tri-block co-polymers as a structure-directing agent during the silica matrix synthesis. The so-obtained mesoporous materials possess significantly larger pores, thicker pore walls and higher hydrothermal stability, in comparison with the analogues materials using alkylammonium-based surfactants [6]. The presence of complementary smaller, disordered micropores in the pore walls is also typical for these materials. These intra-wall pores originate from the interpenetration of the EO-portions of the surfactant into the silica network during synthesis [7]. It was demonstrated that the synthesis approach is very flexible, as the pore shape and interconnectivity of the silicas can be tuned in addition to the pore size by changing the template and/or the synthesis conditions used (silica/template ratio, aging temperature etc.) [8-10].

* Corresponding author: E-mail: fazaeli@iaush.ac.ir
Tel: +98 321 3232706-7; Fax: +98 321 3232701

Hydrogen forms (or free acids) of heteropoly acids (HPAs) usually have low surface areas (the drawback to the $H_3PW_{12}O_{40}$ (PW$_{12}$) and $H_3PMo_{12}O_{40}$ (PMo$_{12}$) is their low surface area, 1-5 $m^2 g^{-1}$, and low porosity, < 0.1 $cm^3 g^{-1}$) [11]. Supported HPA catalysts have much greater surface areas. Many attempts have been made to disperse and fix HPA catalysts on various supports. Support materials such as silica, carbon, and organic resins have been applied with varying levels of success, with new supporting materials and methods being actively pursued. Although the structure and composition of the supported HPAs are sometimes uncertain, high catalytic activities are often observed and separation made easier. For various reasons, such as efficiency, better accessibility to the active sites, cost, *etc*., depositing on a support is currently favoured [12-15].

Oxidation of sulfides is the most straightforward method for the synthesis of sulfoxides and sulfones [16], some examples of which are important as commodity chemicals and, in some cases, as pharmaceuticals [17]. This transformation has been performed in various ways [18-22]. However, the reported methods rarely offer the ideal combination of simplicity of method, rapid and selective reactions, and high yields of products and often suffer from a lack of generality and economical applicability.

Scheme 1.

In this work, mesostructured cellular foam KIT-6 silica was prepared via a surfactant templating method. The KIT-6 silica was then modified by grafting 3-aminopropyl-triethoxysilane (APTES) to create a positive charge on the surface, and thus, to provide sites for the immobilization of $H_3PW_{12}O_{40}$ (denoted by PW_{12}, here after). By taking advantage of the overall negative charge of $[PW_{12}O_{40}]^{3-}$, the $H_3PW_{12}O_{40}$ catalyst was chemically immobilized on the surface modified silicas as a charge matching component. The characteristics of the $H_3PW_{12}O_{40}$ catalyst immobilized on the APTES-modified silica (PW_{12}-APTES@ KIT-6) was extensively investigated.

Herein, we report on the catalytic behavior of PW_{12}-APTES@ KIT-6 for the selective oxidation of sulfides to sulfoxides and sulfones (Scheme 1).

2. Experimental

All materials were commercial reagent grade. Infrared spectra (400–4000 cm^{-1}) were recorded from KBr pellets on a PerkinElmer Spectrum 65 spectrometer. The X-ray powdered diffraction patterns were performed on a Bruker-D8ADVANCE with automatic control. The patterns were run with monochromatic Cu Kα (1.5406 Å) radiation with a scan rate of 2° min^{-1}. Nitrogen adsorption measurements were performed at −196 $^\circ$C by using an ASAP 2010M surface analyzer, and the pretreatment temperature was 180 $^\circ$C. Transmission electron micrographs (TEM) were obtained on a Joel JEM 2010 scan-transmission electron microscope. The sample for the TEM measurement was suspended in ethanol and supported on a carbon coated copper grid.

2.1. Synthesis of mesoporous KIT-6 silica mesoporous

Pure siliceous KIT-6 was prepared according to the previous work by Kleitz et al. [23,24]. A mixture of Pluronic P123 triblock copolymer and n-butanol was as a structure-directing mixture. The molar composition of the starting reaction mixture was P123:TEOS: n-butanol:HCl:H$_2$O= 0.017:1.2:1.31:1.83:195.

Preparation of the large-pore cubic Ia3hd mesoporous silica was as follows: P123 was dissolved in distilled water and 37 wt% HCl solution with stirring at 308 K, and then n-butanol was added. After 1 h stirring, TEOS was added to the homogeneous clear solution. This mixture was left under vigorous and constant stirring at 308K for 24 h. And then it aged at 373K for 24 h under static conditions. The white precipitated product was filtered hot without washing and dried under vacuum at 323K overnight. Surfactant template was removed by refluxing with HCl–ethanol solution (1 g of sample in 150 ml ethanol and 3.8 g 37% HCl) at 323K for 6 h. This procession was repeated thrice.

2.2. Surface modification of KIT-6

Scheme 2 shows the procedures for the surface modification of mesoporous silica KIT-6. Surface modification of mesoporous silica was done by a grafting method [25]. To a suspension of 10 g of calcined mesoporous silica in 50 ml dry toluene, 2.68 g of 3-aminopropyl triethoxy silane was added slowly and heated to reflux with continuous stirring for 8 h under nitrogen atmospheres. The powdery sample containing amino groups was filtered, washed with acetone and then soxhlet extracted using a solution mixture of diethyl ether and dichloromethane (1:1) for 24 h and dried under vacuum. It was finally calcined at 180 ◦C for 2 h to yield the APTES@ KIT-6.

2.3. Immobilization of $H_3PW_{12}O_{40}$ on the APTES@PW$_{12}$

Immobilization of PW_{12} on the APTES@ mesoporous silica (scheme 3) was achieved as following. APTES@ KIT-6 (1.0 g) was added into the acetonitrile solution containing 0.5 g of PW_{12} with vigorous stirring at room temperature, and the resulting solution was maintained at room temperature for 24 h. The solid product was filtered, and then it was dried overnight at 80 ◦C to yield the PW_{12}-APTES@KIT-6 [34].
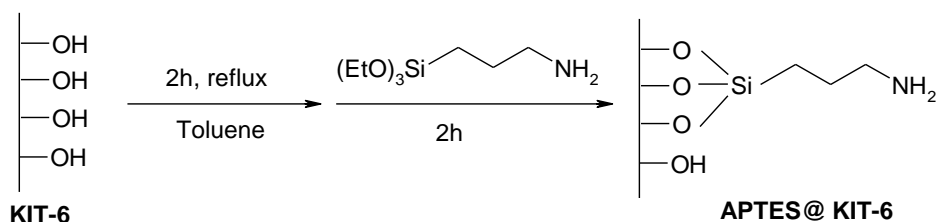
Scheme 2. The procedures for the surface modification of KIT-6.

2.4. Synthesis of sulfoxides and sulfones

To a stirred suspension of the selected sulfide (1 mmol) and the heterogeneous catalyst PW_{12}-APTES@KIT-6 (3 mol%) in ethanol (5 ml), H_2O_2 (15 mmol) was added in one portion. The slurry was stirred at room temperature. The catalyst was filtered off and washed with methanol (5 ml). Ethyl acetate (5 ml) was added and resulting solution was dried with anhydrous sodium sulphate and evaporated in vacuo to afford the crude product which was purified by column chromatography on silica gel (10% EtOAc in hexane) to afford the pure sulfoxide. Similar method was utilized to produce sulfones. In this case 5 mol % of PW_{12}-APTES@KIT-6 in CH_3CN were utilized.

2.5. Selected spectral data

Dibutyl sulfoxide (2a): mp 34-35°C. ^1H NMR (400 MHz, $CDCl_3$) δ: 0.97 (t, 6H, *J*=7.4 Hz), 1.41-1.57 (m, 4H), 1.72-1.79 (m, 4H), 2.60-2.73 (m, 4H). ^{13}C NMR (100 MHz, $CDCl_3$) δ: 13.64, 22.05, 24.56, 52.13.

Methyl phenyl sulfoxide (2b): mp 30-31°C. IR (v_{max}, KBr, cm^{-1}): 530, 690, 751, 957, 1037, 1431, 1647, 2922, 3004; ^1H NMR (400 MHz, $CDCl_3$) δ: 2.73 (s, 3H), 7.49-7.57 (m, 3H), 7.61-7.67 (m, 2H). ^{13}C NMR (100 MHz, $CDCl_3$) δ: 43.95, 123.47, 129.33, 131.00, 145.72.

Diphenyl sulfoxide (2c): mp 72-73°C. ^1H NMR (400 MHz, $CDCl_3$) δ: 7.42-7.49 (m, 6H), 7.63-7.66 (m, 4H). ^{13}C NMR (100 MHz, $CDCl_3$) δ: 124.77, 129.30, 131.03, 145.61.

Benzyl 4-bromobenzyl sulfoxide (2d): mp 139-140°C. IR (v_{max}, KBr, cm^{-1}): 1028; ^1H NMR (400 MHz, $CDCl_3$) δ: 3.78(d, 1H, *J*= 13.1 Hz), 3.89(d, 1H, *J*= 13.09 Hz), 3.95 (s, 2H), 7.2 (d, 2H, *J*=8.3 Hz), 7.32-7.33 (m, 2H), 7.40-7.44 (m, 3H), 7.54(d, 2H, *J*=8.3 Hz).

4-Nitrobenzyl phenyl sulfoxide (2e): mp 161-163°C. IR (v_{max}, KBr, cm^{-1}): 1026, 1345, 1515; ^1H NMR (200 MHz, $CDCl_3$) δ: 4.04 (d, 1H, *J*= 12.0 Hz), 4.24 (d, 1H, *J*= 12.0 Hz), 7.13 (d, 1H, *J*= 6.5 Hz), 7.40-7.51 (m, 5H), 8.12 (d, 2H, *J*= 6.5 Hz).

Methyl 2-(phenylsulfinyl)acetate (2j): Isolated as yellow oil. IR (v_{max}, KBr, cm^{-1}): 487, 691, 749, 1045,

1444, 1736, 2927; ^1H NMR (400 MHz, $CDCl_3$) δ: 3.72 (s, 3H), 3.68(d, 1H, *J*= 13.6 Hz), 3.86 (d, 1H, *J*= 13.6 Hz), 7.52-7.59 (m, 3H); 7.66-7.73 (m, 2H).

Dibutyl sulfone (3a): mp 46-47°C. ^1H NMR (400 MHz, $CDCl_3$) δ: 0.97 (t, 6H, *J*=7.4 Hz), 1.44-1.53 (m, 4H), 1.78-1.86 (m, 4H), 2.93-2.97 (m, 4H). ^{13}C NMR (100 MHz, $CDCl_3$) δ: 13.53, 21.78, 23.93, 52.46.

Methyl phenyl sulfone (3b): mp 89-90°C. ^1H NMR (400 MHz, $CDCl_3$) δ: 3.06 (s, 3H), 7.56-7.60 (m, 2H), 7.65-7.69 (m, 1H), 7.95-7.97 (m, 2H). ^{13}C NMR (100 MHz, $CDCl_3$) δ: 44.67, 127.32, 129.34, 133.67, 140.58.

Diphenyl sulfone (3c): mp 128-129°C. ^1H NMR (400 MHz, $CDCl_3$) δ: 7.48-7.59 (m, 6H), 7.94-7.97 (m, 4H). ^{13}C NMR (100 MHz, $CDCl_3$) δ: 127.65, 129.26, 133.15, 141.61.

Benzyl 4-bromobenzyl sulfone (3d): mp 176-178°C. IR (v_{max}, KBr, cm^{-1}): 1116, 1299; ^1H NMR (400 MHz, $CDCl_3$) δ: 4.02 (s, 2H), 4.14 (s, 2H), 7.17-7.60 (m, 9H).

4-Nitrobenzyl phenyl sulfone (3e): mp 204-205°C. IR (v_{max}, KBr, cm^{-1}): 1140, 1302, 1341, 1519; ^1H NMR (400 MHz, $CDCl_3$) δ: 4.44 (s, 2H), 7.10 (d, 2H, *J*= 6.5 Hz), 7.40-7.70 (m, 5H), 8.18 (d, 2H, *J*= 6.5 Hz).

2-Hydroxyethyl phenyl sulfone (3k): ^1H NMR (400 MHz, $CDCl_3$, δ): 2.04 (br, 1H), 3.35 (t, 2H, *J*= 5.2 Hz), 4.01 (t, 2H, *J*= 5.2 Hz), 7.60 (t, 2H, *J*= 7.6 Hz), 7.68-7.72 (m, 1H), 7.95 (d, 2H, *J*= 7.6 Hz). ^{13}C NMR (100 MHz, $CDCl_3$) δ: 56.33, 58.24, 127.95, 129.47, 134.07, 138.94.

3. Results and Discussion

3.1. Structural characterization

3.1.1. FTIR

Fig. 1 presents the FTIR spectra in the skeletal region of 4000–400 cm^{-1} for the bare and modified KIT-6. A band at 1635-1647 cm^{-1} observed in all samples can be assigned to the –OH vibration of physisorbed H_2O. In the case of unmodified KIT-6, the Si–O–Si bands originated from silicas were observed at around 1000–1250, 805, and 474 cm^{-1}. The amino functionalization followed by succinylation of the mesoporous silicas
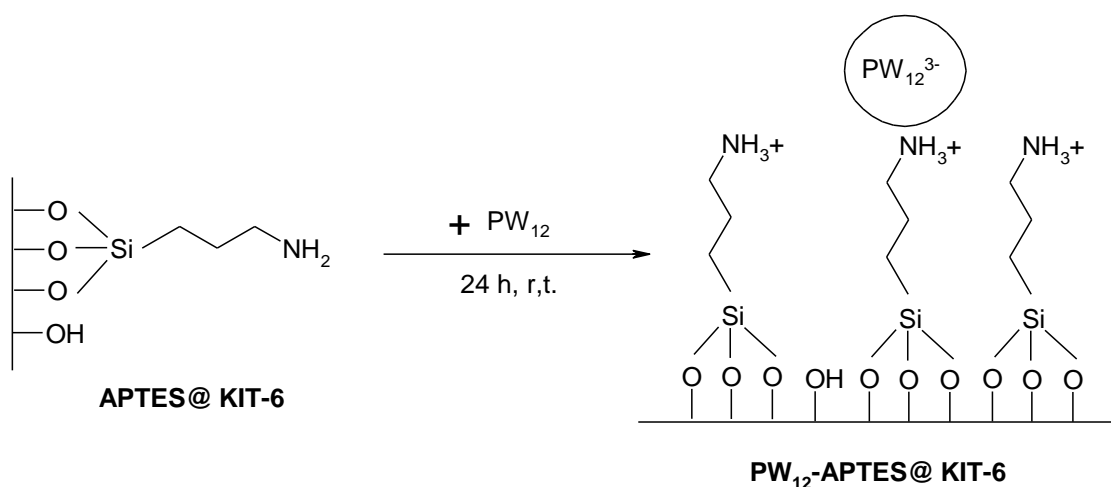
Scheme 3. The procedures for the immobilization of PW_{12} on the surface APTES@KIT-6.

(APTES@KIT-6) was analyzed by FTIR spectroscopy. The broad band at 3600–3000cm^{-1} for hydrogen bonded silanol [26,27] was appreciably reduced in the modified samples. The organosilane presence was identified by the absorbance of the band 2950–2850cm^{-1} for the propyl chain [28] and the deformation bands at 1489 cm^{-1} [27]. The N-H absorption band overlapped with O-H bands at 3439 cm^{-1} [26]. The presence of bands at 1585 (NH amide II band) and 1415–1419 cm^{-1} (-C-N amide) confirmed that succinylation had taken place [28,29]. The successful immobilization of the PW_{12} catalyst on the aminopropyl-functionalized mesoporous silicas were confirmed by FT-IR analyses as shown in Fig. 1. The primary structure of unsupported PW_{12} can be identified by the four characteristic IR bands appearing at 1083 cm^{-1} (P–O band), 964 cm^{-1} (W=O band), 890 and 809 cm^{-1} (W–O–W bands) [30]. The characteristic IR bands of PW_{12} in the PW_{12}/APTES@ KIT-6 were different from those of unsupported PW_{12}. The P–O band in the PW_{12}/APTES@ KIT-6 sample was not clearly identified due to overlap by the broad Si–O–Si band. However, W=O and W–O–W bands of PW_{12} in the PW_{12}-APTES@KIT-6 appeared at slightly shifted positions compared to those of the unsupported PW_{12}, indicating a strong interaction between PW_{12} and APTES@ KIT-6 [31].

3.1.2. XRD

Fig. 2 shows the XRD patterns of the PW_{12}-APTES@KIT-6 within the 2θ range of 0.7–10° (a) and 0.7–10° (b). XRD patterns of parent KIT-6 materials represent two well distinguished reflections in the small-angle region, which could be assigned to the (2 1 1) and (2 2 0) planes of 3D cubic structure [32]. After immobilization of PW_{12}-APTES, the intensities of the reflections decrease, which could be assigned to the decrease in electron density contrast upon

introduction of PW_{12}-APTES into the mesoporous of the KIT-6 host materials.

Fig. 2b shows the XRD patterns of PW_{12}-APTES@KIT-6 in (2θ= 10-80°). What is interesting is that all samples showed no characteristic XRD pattern, even though 35% wt% PW_{12} was loaded on the mesoporous silicas. This indicates that the PW_{12} species were not in a crystal state but in an amorphous-like state, demonstrating that Keggin species are finely and molecularly dispersed on the mesoporous silicas.
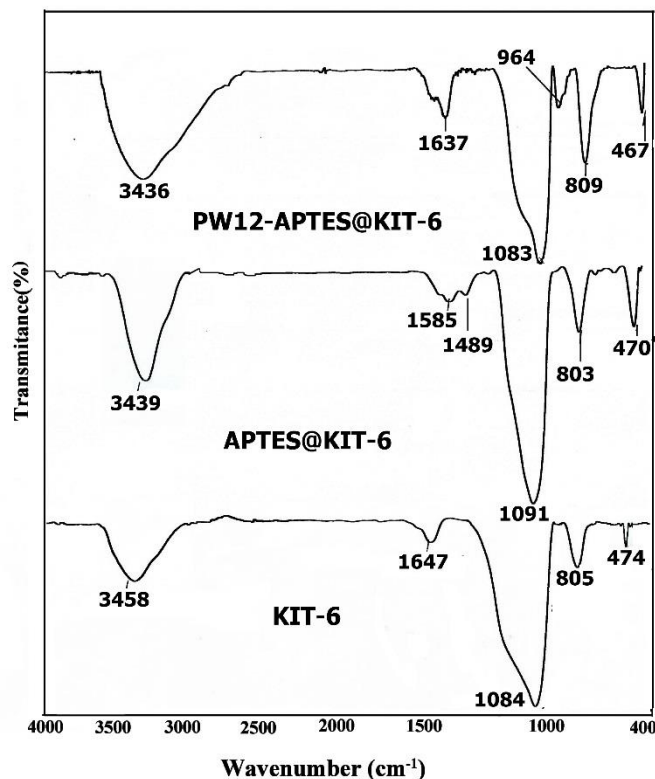

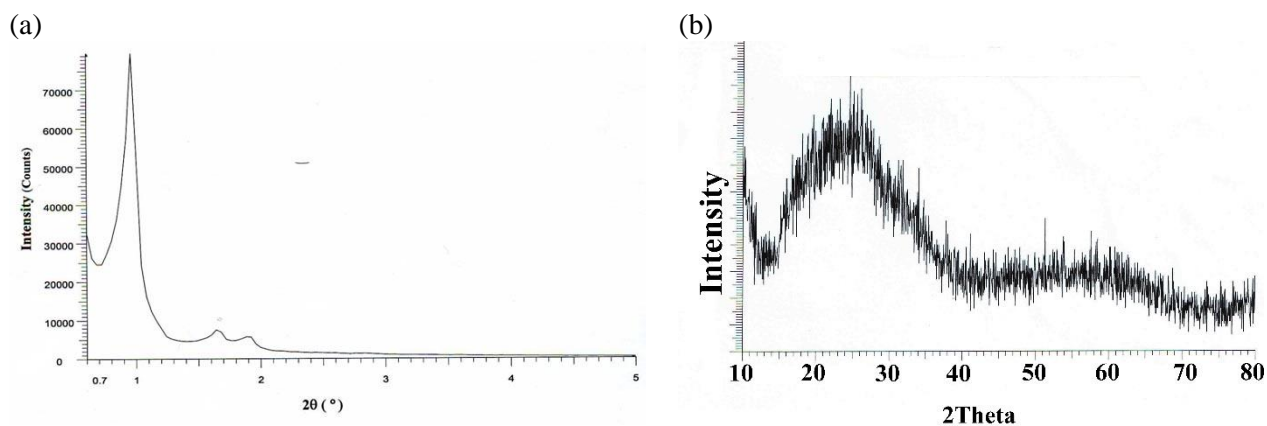**Fig. 1.** FTIR spectra of KIT-6 materials.

(a)

(b)

Fig. 2. XRD patterns of PW_{12}/ APTES@KIT-6 (a) 2θ=0.7-10; (b) 2θ=10-80.

3.1.3. N_2 adsorption–desorption isotherms

Fig. 3 shows the N_2 adsorption–desorption isotherms and pore size distributions of the bare KIT-6 and PW_{12}-APTES@KIT-6. All the samples exhibited typical IV type isotherms and H1 type hysteresis loops at high relative pressures according to the IUPAC nomenclature [33], which are the typical characteristics of mesoporous materials [34-36]. This indicates that PW_{12}-APTES@KIT-6 with large pore size distribution were successfully prepared. Interestingly, the PW_{12}-APTES@KIT-6 showed very similar isotherm pattern and pore size distribution (Fig. 3b) compared to KIT-6, indicating that the mesopore structure of KIT-6 was still maintained even after the surface modification step and the subsequent immobilization step of PW_{12}. Physical Properties of KIT-6, PW_{12} (bulk) and PW_{12}-APTES@KIT-6 are listed in Table 1. As expected, the BET surface areas and total pore volumes of unmodified MCF, SBA-15 and KIT-6 are decreased after the functionalization with PW_{12}. These changes reflect that part of the

mesopore volume in the KIT-6 matrix is filled with PW_{12}.

3.1.4. TEM

Fig. 4 shows the TEM images of PW_{12}-APTES@KIT-6. The sample for the TEM measurement was suspended in ethanol and supported on a carbon coated copper grid. PW_{12}-APTES@KIT-6 catalyst exhibited a disordered pore structure with large pores in the range of 10-15 nm. In all samples, a well-resolved contrast characteristic of certain silica mesopore structure symmetry is still observed, which is an indication for the preservation of the long ordered arrangement of the channels in the silica host matrix after the PW_{12} deposition. The places with darker contrast could be assigned to the presence of PW_{12} particles with different dispersion. The small dark spots in the images could be ascribed to PW_{12} particles, probably located in to the support channels. The larger dark areas over the channels most likely correspond to PW_{12} agglomerates on the external surface [37,38].
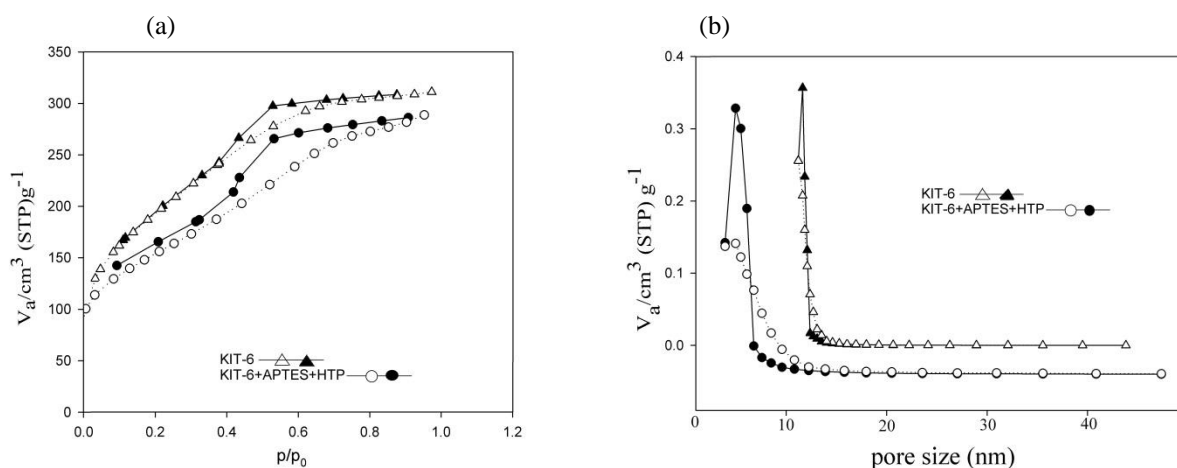
(a)

(b)

Fig. 3. N_2-adsorption-desorption isotherms (left) and pore size distributions calculated by the BJH method (right) of bare KIT-6 and PW_{12}-APTES@KIT-6.

Table 1. The texture parameters of bare KIT-6 and PW_{12}-APTES@KIT-6 in comparison with the bulk PW_{12} materials.

Entry	Sample	BET, surface area (m^2/g)	Pore volume (cm^3/g)	Pore diameter (nm)
1	KIT-6, silica	697	0.48	2.8
2	PW_{12}	6	-	-
3	PW_{12}- APTES@ KIT-6	212	0.18	0.34

3.2. Catalytic activity

The oxidation of PhSMe using H_2O_2 which did not proceed in the absence of catalyst under mild conditions was used as a model reaction. To find optimum reaction conditions, the influence of different factors affecting the conversion and selectivity of the oxidation reaction such as catalyst concentration, solvent nature and the molar ratio of H_2O_2/sulfide, were investigated in this study. It was observed that the highest yield and selectivity to sulfoxide were achieved in the presence of 3 mol% of the catalyst within 2h. Also an increase in the catalyst/sulfide molar ratio up to 20 mol% does not affect the reaction rate and yield of sulfoxide product in this catalytic system (Table 2).

The influence of solvent nature on the selectivity and reaction rate in this reaction system was also studied. From the examination of five reaction solvents such as dichloromethane, acetone, acetonitrile, methanol and ethanol in this catalytic reaction, it was observed that two protic solvents, methanol and especially ethanol, significantly enhanced the yield and the selectivity of sulfoxide product. The eco-friendly property of ethanol strongly induced us to employ it as the reaction solvent in this oxidation system.
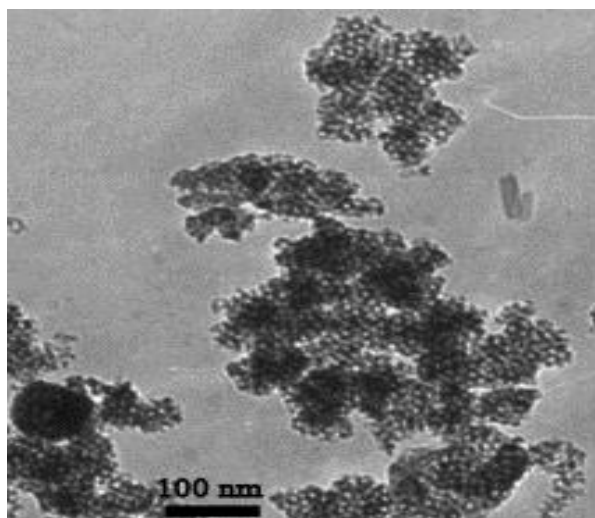
Fig. 4. TEM images of PW_{12}/APTES@KIT-6.

The applicability of the H_2O_2/ PW_{12}-APTES@KIT-6 systems was then examined for the sulfoxidation of diaryl, dibenzyl, aryl benzyl, dialkyl and cyclic sulfides in methanol at room temperature. A ratio of 1:15:3 sulfide:H_2O_2: PW_{12}-APTES@KIT-6 was found to be optimum for complete conversion of sulfides to sulfoxides and the results are presented in Table 3. As shown, all the reactions were complete within a very short time and the sulfoxides were obtained in almost quantitative yields as the sole oxidation products. The chemoselectivity is noteworthy. Under such conditions, the sulfide function was highly reactive, and various other functional groups such as alkenes and a ketone were tolerated.

In order to demonstrate the efficiency and applicability of the H_2O_2/ PW_{12}-APTES@KIT-6 system further, the chemoselective oxidation of sulfides to sulfones was also investigated. The reaction conditions specified in Table 3 were optimized for carrying out the reaction in CH_3CN at room temperature (sulphide:H_2O_2: PW_{12}-APTES@KIT-6 ratio = 1:15:5).

It was found that a wide variety of diaryl, dialkyl, dibenzyl, aryl benzyl, alkyl aryl and cyclic sulfides were oxidized to their corresponding sulfones in excellent yields in CH_3CN at room temperature. The results are summarized in Table 3.

In order to show the merit of the present work in comparison with recently reported protocols, we compared the results with respect to the amounts of the catalysts used, reaction times and yields of the products (Table 4). Comparison of PW_{12}-APTES@KIT-6 with these catalysts for selective oxidation of sulfides to sulfoxides show that activity of PW_{12}-APTES@KIT-6 seems to be higher than or equal with other known catalysts (Table 4).

3.2.1. Reusability

Apart from presenting a good catalytic activity, long-term stability and the absence of leaching are of primary importance for solid catalysts. The recovery and reusability of the PW_{12}-APTES@KIT-6 has been also investigated in the oxidation of methyl phenyl sulfide.

Table 2. Effect of different conditions in the oxidation of methyl phenyl sulfides to sulfoxides after 2h.

Entry	Solvent	Catalyst (mol %)	H_2O_2/sulfide	Yield (%)[a]
1	dichloromethane	3	15	23
2	acetone	3	15	41
3	acetonitrile	3	15	55
4	methanol	3	15	78
5	ethanol	3	15	98
6	ethanol	2	15	75
7	ethanol	4	15	98
8	ethanol	3	12	82
8	ethanol	3	20	86

[a]Isolated Yield.

Table 3. Oxidation of sulfides to sulfoxides and sulfones using the PW_{12}-APTES@ KIT-6 system.

Sulfide **1**	Sulfoxide **2** Time (min) : Yield[a,c] (%)	Sulfone **3** Time (min) : Yield[b,c] (%)
$(C_4H_9)_2S$ **1a**	60 : 98	90 : 95
$(C_6H_5)SMe$ **1b**	120 : 98	100 : 92
$(C_6H_5)_2S$ **1c**	140 : 95	160 : 95
$(4\text{-}Br\text{-}C_6H_5CH_2) S(CH_2C_6H_5)$ **1d**	155 : 95	100 : 96
$(4\text{-}NO_2\text{-}C_6H_5)S(C_6H_5)$ **1e**	130 : 98	100 : 90
$(4\text{-}Me\text{-}C_6H_5)S(CH_2C_6H_5)$ **1f**	140 : 90	160 : 98
$(4\text{-}Me\text{-}C_6H_5)S(CH_2C_6H_5\text{-}4\text{-}Br)$ **1g**	150 : 92	100 : 98
$(C_6H_5)S(CH_2C_6H_5)$ **1h**	120 : 98	170 : 90
$(C_6H_5)S(C_3H_5)$ **1i**	115 : 98	160 : 92
$(C_6H_5)S(CH_2\text{-}COOMe)$ **1j**	110 : 87	155 : 92
$(C_3H_5)S(C_3H_5)$ **1k**	80 : 90	80 : 92

[a] Reaction conditions: Sulfide (1 mmol), H_2O_2 (15 mmol), PW_{12}-APTES@KIT-6 (3 mol%), EtOH (5 ml), r.t.
[b] Reaction conditions: Sulfide (1 mmol), H_2O_2 (15 mmol), PW_{12}-APTES@KIT-6 (5 mol%), CH_3CN (5 ml), r.t.
[c]Isolated yields.

Table 4. Comparison of PW_{12}-APTES@KIT-6 with some other catalyst for oxidation of PhSMe.

Entry	Reagent	Conditions	Time (h)	Yield (%)[a]	Ref.
1	N_2O_4/Charcoal	CH_2Cl_2, r.t.	3	93	[39]
2	Mont. K10/H_2O_2 (35%)	MeOH, r.t	2.5	95	[40]
3	$HAuCl_4.4H_2O$	r.t.	1	92	[43]
4	Cyclohexylidenebishydroperoxide	CH_2Cl_2, r.t.	0.5	89	[44]
5	Cinchonine $CinH_3PMo_{12}O_{40}$ ($PM_{12}Cin$)	CH_3CN, 20 ^{o}C	2	95	[46]
6	BisILs-C_8H_{17}-W2[a]	MeOH/CH_2Cl_2, 25 ^{o}C	1.5	95.5	[47]
7	PW_{12}-APTES@KIT-6; this work	EtOH, r.t	2	98	-

[a]Yield refers to the corresponding sulfoxide.

The standard procedure, described in the experimental section, was followed to perform the first run. After 2h of reaction, the solid was filtered off and dried for 4 h at 110 ^{o}C and calcined for 4 h at 350 ^{o}C. The products were obtained of the same purity as in the first to fifth runs, but the yields were gradually decreased in runs carried out using recycled catalyst (Fig. 5). It is well-known that due to solubility of HPA in polar solvents, HPA leaching will be significant from HPA/support system. After fifth run, the PW_{12} was leached from the APTES@KIT-6 (proved by atomic absorption) and this led to the deactivation of heterogeneous catalyst. The possible leaching of the active phase was also studied by hot filtration experiments, the catalyst is filtered off during the reaction in the first run and possible catalytic activity in the obtained solution under the same conditions is followed. After hot filtration of the catalyst, no further reaction is observed in the solution, showing the heterogeneous behaviour of the solids. Analysis of the liquid by ICP did not indicate any metal presence.
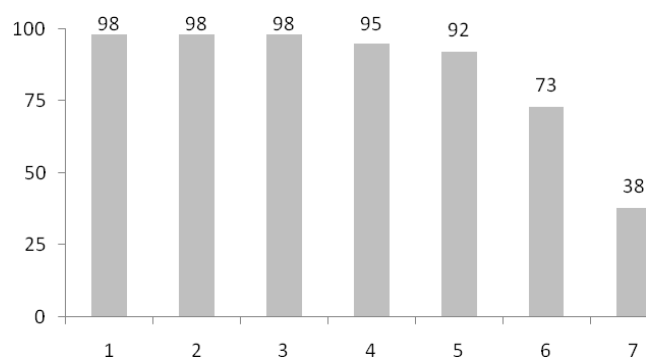

Fig.5. Investigation of the feasibility of reusing PW_{12}-APTES@ KIT-6 in the oxidation of methyl phenyl sulfide to corresponding sulfoxide with H_2O_2 in CH_3CN after 2 h.

4. Conclusions

The results of this research demonstrated that PW_{12}-APTES@KIT-6 is affecting catalyst on the highly chemoselective and rapid oxidation of functionalized sulfides to sulfoxides and sulfones with H_2O_2 under mild conditions. From the characterization of catalyst, it showed that the structure of PW_{12} remained intact, and PW_{12} was distributed on KIT-6 mesoporous silica support evenly. It is noteworthy that the reaction tolerates oxidatively sensitive functional groups and the sulfur atom is selectively oxidized.

Acknowledgment

References

[1] A.Taguchi, F. Schuth. Microporous Mesoporous Mater. 77 (2005) 1-45.

[2] T. Tsoncheva, J. Rosenholm, C. V. Teixeira, M. Dimitrov, M. Linden, C. Minchev, Microporous Mesoporous Mater. 89 (2006) 209-218.

[3] T. Tsoncheva, J. Rosenholm, M. Linden, L. Ivanova, C. Minchev, Appl. Catal. A: Gen. 318 (2007) 234-243.

[4] T. Tsoncheva, Tz. Venkov, M. Dimitrov, C. Minchev, K. Hadjiivanov, J. Mol. Catal. A: Chem. 209 (2003) 125-134.

[5] R. Kohn, D. Paneva, M. Dimitrov, T. Tsoncheva, I. Mitov, C. Minchev, M. Froba, Microporous Mesoporous Mater. 63 (2003) 125-137.

[6] S. Forster, Top. Cur. Chem. 226 (2003) 1-28.

[7] P. L. Ravikovitch, A. V. Neimark, J. Phys. Chem. B. 105 (2001) 6817-6823.

[8] M. Choi, W. Heo, F. Kletiz, R. Ryoo, Chem. Commun. (2003) 1340-1341.

[9] F. Kletiz, S. H. Choi, r. Ryoo. Chem. Commun. (2003) 2136-2137.

[10] F. Kletiz, T. W. Kim, R. Ryoo, Langmuir 22 (2006) 440-445.

[11] I.V. Kozhevnikov, Catalysis by Polyoxometalates, Wiley, England, 2002.

[12] R. Fazaeli, S. Tangestaninejad, H. Aliyan, M. Moghadam, Appl. Catal. A: Gen. 309 (2006) 44-51.

[13] R. Fazaeli, S. Tangestaninejad, H. Aliyan Appl. Catal. A: Gen. 318 (2007) 218-226.

[14] R. Fazaeli, H. Aliyan, Appl. Catal. A: Gen. 331 (2007) 78-83.

[15] R. Fazaeli, H. Aliyan, Appl. Catal. A: Gen. 353 (2009) 74-79.

[16] The Synthesis of Sulphones, Sulphoxides, and Cyclic Sulphides; Patai, S., Rappoport, Z., Eds.; Wiley: New York, 1994.

[17] Clark, E. In Kirk–Othmer Encyclopedia of Chemical Technology, 4th ed; Kroschwitz, J. I., Howe-Grant, M., Eds.; Wiley: New York, 1997; Vol. 23, pp 134–146.

[18] X. Shi, X. Han, W. Ma, J. Wei, J. Li, Q. Zhang, Z. Chen, J. Mol. Catal. A: Chem. 341 (2011) 57–62.

[19] P. Ballistreri, F.G. Fortuna, C. Pappalardo, A.A. Tomaselli, G.M. Toscano, R. J. Mol. Catal. A: Chem. 308 (2009) 56–60.

[20] N. Gharah, S.K. Chakraborty, A. Mukherjee, R. Bhattacharyya, Inorg. Chim. Acta 362 (2009) 1089–1100.

[21] I. Sheikhshoaie, A. Rezaeifard, N. Monadi, S. Kaafi, Polyhedron 28 (2009) 733–738

[22] H. Egami, T. Katsuki. J. Am. Chem. Soc. 129 (2007) 8940-8941.

[23] F. Kleitz, S.H. Choi, R. Ryoo, Chem. Commun. (2003) 2136–2137.

[24] T.W. Kim, F. Kleitz, B. Paul, R. Ryoo, J. Am. Chem. Soc. 127 (2005) 7601–7610.

[25] V.D. Chaube, S. Shylesh, A.P. Singh, J. Mol. Catal: A: Chem. 241 (2005) 79–87.

[26] I. Diaz, C. Marquez-Alvarez, F. Mahino, J. Perez-Periente, E. Sastre, J. Catal. 193 (2000) 283–294.

[27] B.H. Wouters, T. Chen, M. Dewilde, P.J. Grobet, Micropor. Mesopor. Mater. 44–45 (2001) 453–457.

[28] A.B. Jarzębski, K. Szymanska, J. Bryjak, J. Mrowiec-Białoń, Catal. Today 124 (2007) 2–10.

[29] J. Aburto, M. Ayala, I. Bustos-Jaimes, C. Montiel, E. Terres, J.M. Domınguez, E. Torres, Micropor. Mesopor. Mater. 83 (2005) 193–200.

[30] I.V. Kozhevnikov, Catalysis by Polyoxometalates, Wiley, England, 2002.

[31] V.D. Chaube, S. Shylesh, A.P. Singh, J. Mol. Catal. A: Chem. 241 (2005) 79–87.

[32] A. Prabhu, L. Kumaresan, M. Palanichamy, V. Murugesan, Appl. Catal. A: Chem. 360 (2009) 59-65.

[33] K.S.W. Sing, D.H. Everett, R.A.W. Haul, L. Moscou, R.A. Pierotti, J. Rouquerol, Pure Appl. Chem. 57 (1985) 603-619.

[34] J.S. Beck, J.C.Vartuli, W.J. Roth, M.E. Leonowicz, C.T. Kresge, K.D. Schmitt. J. Am. Chem. Soc. 114 (1992) 10834-10843.

[35] C.T. Kresge, M.E. Leonowicz, W.J. Roth, J.C. Vartuli, J.S. Beck. Nature 359 (1992) 710-712.

[36] M. Che, J.C. Védrine, Characterization of solid materials and heterogeneous catalysts: From structure to surface reactivity" Wiley-VCH April 2012, 853-879.

[37] T. Tsoncheva, L. Ivanova, J. Rosenholm, M. Linden, Appl. Catal. B: Env. 89 (2009) 365-374.

[38] D. G. Castner, Ph. R. Watson, I. Y. Chan, J. Phys. Chem. 93 (1989) 3188-3194.

[39] N. Iranpoor, H. Firouzabadi, A.R. Pourali, Synlett (2004) 347-349.

[40] M.M. Lakouraj, M. Tajbakhsh, H. Tashakkorian, Lett. Org. Chem. 4 (2007) 75-79.

[41] R. Das, D. Chakraborty, Tetraheron Lett. 51 (2010) 6255-6258.

[42] Y. K. Hwang, D.-Y. Hong, J.-S. Chang, H. Seo, M. Yoon, J. Kim, S. H. Jhung, C. Serre, G. Fe´rey, Appl. Catal. A: Gen. 358 (2009) 249–253.

[43] Y. Yuan, Y. Bian, Tetrahedron Lett. 48 (2007) 8518-8520.

[44] S.V. Suresh, K. Rajesh, D.C. Babu, N. Suryakiran, Y. Venkateswarlu, Tetrahedron Lett. 49 (2008) 3463-3465.

[45] S. Kumar, S. Verma, S.L. Jain, B. Sain, Tetrahedron Lett. 52 (2011) 3393-3396.

[46] A. G. Sathicq, G. P. Romanelli, V. Palermo, P. G. Vazquez, H. J. Thomas, Tetrahedron Lett. 49 (2008) 1441–1444.

[47] X. Shi, X. Hana, W. Ma, J. Weia, J. Li, Q. Zhang, Z. Chen, J. Mol. Catal. A: Chem. 341 (2011) 57–62.